Transmission properties of time-dependent one-dimensional metamaterials

H. Ammari and J. Cao and L. Rueff

Research Report No. 2023-09
January 2023

Seminar für Angewandte Mathematik
Eidgenössische Technische Hochschule
CH-8092 Zürich
Switzerland

Funding SNF: 200021--200307

Transmission properties of time-dependent one-dimensional metamaterials *

Habib Ammari[†] Jinghao Cao[†] Liora Rueff[†]

Abstract

We solve the wave equation with periodically time-modulated material parameters in a one-dimensional high-contrast resonator structure in the subwavelength regime exactly, for which we compute the subwavelength quasifrequencies numerically using Muller's method. We prove a formula in the form of an ODE using a capacitance matrix approximation. Comparison of the exact results with the approximations reveals that the method of capacitance matrix approximation is accurate and significantly more efficient. We prove various transmission properties in the aforementioned structure and illustrate them with numerical simulations. In particular, we investigate the effect of time-modulated material parameters on the formation of degenerate points, band gaps and k-gaps.

Mathematics Subject Classification (MSC2000): 35J05, 35C20, 35P20, 74J20

Keywords: wave manipulation at subwavelength scales, unidirectional wave, subwavelength quasifrequency, space-time modulated medium, metamaterial, non-reciprocal band gap, k-gap

1 Introduction

Numerous papers have tackled the problem of understanding and manipulating wave propagation in two- and three-dimensional systems with subwavelength resonant structures [5, 24, 31]. Systems of subwavelength resonant structures are of particular interest due to their ability to manipulate waves at subwavelength scales in two- and three-dimensional materials [26–28]. Such media are made up of a background medium and highly contrasting inclusions, which we call *subwavelength resonators*. The fact that these inclusions are highly contrasting leads to *subwavelength resonances*, frequencies at which the resonators interact with incident waves with wavelengths of possibly larger magnitudes [22]. This kind of structure appears in various application areas. Subwavelength resonances in highly contrasted structures can be found, for instance, in elastic media [20, 29], in plasmonic particles [15, 17–19], Helmholtz resonators [16, 27] and in dielectric high-index particles [14, 32]. The plethora of applications of subwavelength resonances make this topic of more general scientific interest.

Wave propagation through a two- or three-dimensional structure with highly contrasting resonators is modelled by a *high-contrast Helmholtz problem* [7]. It has been shown that the high material contrast within the structure is a key assumption for the existence of resonant behaviours at subwavelength scales [9, 33]. The way the aforementioned Helmholtz problem is approximately solved is to use single-layer potentials based on the fundamental solution of the Laplace problem [10]. Specifically, single-layer potentials are used to derive the so-called

*This work was supported in part by the Swiss National Science Foundation grant number 200021–200307.
†Department of Mathematics, ETH Zürich, Rämistrasse 101, CH-8092 Zürich, Switzerland (habib.ammari@math.ethz.ch, jinghao.cao@sam.math.ethz.ch, liora.rueff@sam.math.ethz.ch).

capacitance matrix, which is used to approximate the differential equations in terms of a discrete eigenvalue problem [5].

Analogously to the two- and three-dimensional cases, the wave propagation in a one-dimensional structure is modelled by a Helmholtz problem [22]. However, we note that layer potential techniques cannot be applied to the one-dimensional setting. Thus, we must derive a distinct method to approximately solve the one-dimensional problem, which has previously been done for the finite one-dimensional case in [22]. Therefore, the results obtained in higher dimensions are not bound to hold true in the one-dimensional case, which motivates this work. Here, we seek to find a capacitance matrix approximation to the subwavelength quasifrequencies for which the quasi-periodic one-dimensional problem attains a non-trivial solution; see Definition 3.2. Using such discrete approximation we shall be able to reproduce a number of phenomena induced by time-modulated material parameters in higher dimensional structures.

Many intriguing phenomena have been shown in two- and three-dimensional high-contrast metamaterials, however, not in the one-dimensional setting. The interest in the one-dimensional case has recently risen because, in contrast to higher-dimensional cases, interactions between the resonators in one-dimensional systems only imply the nearest neighbors. The capacitance matrix formalism used for analysing systems of subwavelength resonators in one dimension corresponds to the tight-binding approximation for quantum systems while in three dimensions some correspondence holds only for dilute resonators [8]. Consequently, the one-dimensional case connects the field of high-contrast metamaterials to condensed-matter theory better.

Relevant recent works which focus on one-dimensional subwavelength resonators are [22] and [1]. While [22] presents the mathematical theory for the case of finitely many resonators aligned in one dimension, [1] considers the existence and characterization of topologically protected edge modes arising from defects in the periodicity of a chain of subwavelength resonators. Further relevant research has been conducted for the case of one-dimensional chains of resonators contained within a three-dimensional background medium in [6, 7]. Moreover, in [30] the authors considered topological photonic materials in one dimension, but they look at the consequences certain topological properties have, but not at the formation of *band gaps* and *non-reciprocity.*

This paper particularly introduces periodically time-modulated material parameters in a quasi-periodic system of resonators, which is a natural extension to already known behaviours in one-dimensional subwavelength structures. The analogue setting in higher dimensions has been well-studied in [2–4, 13]. We aim to investigate the formation of band gaps, which is a regime of subwavelength frequencies with which waves are unable to propagate through the medium, and they exponentially decay instead [4]. It has been proven in higher dimensions that the time-modulation of the material's density leads to the emergence of band gaps [4]. On the other hand, the time-modulation of the material's bulk modulus leads to *k-gaps* [4]. The so-called k-gaps are known as band gaps in the momentum variable [13]. Additionally, time-modulated material parameters induce non-reciprocity of waves propagating through two- or three-dimensional materials [4, 13, 23, 36]. This non-reciprocity can be used to replicate spin effects from quantum systems [3, 13, 35] and to show that the unidirectional guiding phenomenon is not particular to quantum systems [25, 34]. The understanding of the coupling between time-modulated material parameters and the occurrence of band gaps, k-gaps and non-reciprocity is meaningful to the field of metamaterials. In this paper we aim to prove these three observances in the case of a one-dimensional periodic structure.

We start by providing an overview of the problem setting and introduce the governing equations in the form of a modified Helmholtz equation with suitable boundary conditions in Section 2. We particularly assume quasi-periodicity of the problem and the material parameters to be periodically time-modulated, which makes a new contribution to the understanding of subwavelength resonance phenomena in one dimension. In Section 3 we introduce a scheme to solve the governing equations exactly in order to find the subwavelength quasifrequencies, for which we make use of the Dirichlet-to-Neumann approach. In Section 4 we provide a brief explanation of Muller's method - the root-finding algorithm used to solve the modified Helmholtz equations. In Section 5 we shift our attention to a further novel contribution of this paper, which consists of the introduction of a capacitance matrix approximation of the subwavelength quasifrequencies. We prove that such a discrete approximation is a suitable replacement for the numerical scheme solving the wave problem exactly. Lastly, we move on to apply the capacitance matrix approximation to investigate the formation of band gaps, k-gaps and degeneracies and analyze the reciprocity of the wave propagation in Section 6. We summarize our results in Section 7.

2 Problem formulation and preliminary theory

2.1 Problem formulation

We seek to solve the one-dimensional wave equation on a domain composed of contrasting materials. In this section, we first introduce the setting, which we shall consider in the remainder of this paper. Moreover, we define the material parameters to be time-dependent and assume quasi-periodicity.

We consider the case of a one-dimensional system of periodically reoccurring chains of N disjoint subwavelength resonators $D_i := (x_i^-, x_i^+)$, where $(x_i^\pm)_{1\le i\le N}$ are the $2N$ boundary points of the resonators satisfying $x_i^+ < x_{i+1}^-$, for any $1 \le i \le N-1$. We denote by $(x_i^\pm)_{i\in\mathbb{N}}$ the infinite sequence defined by $x_{i+N}^\pm := x_i^\pm + L$, where $L \in \mathbb{R}_{>0}$ is the period of an infinite chain of resonators. Furthermore, we denote the length of the i-th resonator D_i by $\ell_i := x_i^+ - x_i^-$, and the length of the gap between the i-th and the $(i+1)$-th resonator by $\ell_{i(i+1)} := x_{i+1}^- - x_i^+$. Note that we will use the convention $\ell_{N(N+1)} := x_{N+1}^- - x_N^+ = L - x_N^+ + x_1^-$ throughout this paper. We refer to Figure 1 for an illustration of the hereby introduced setting.

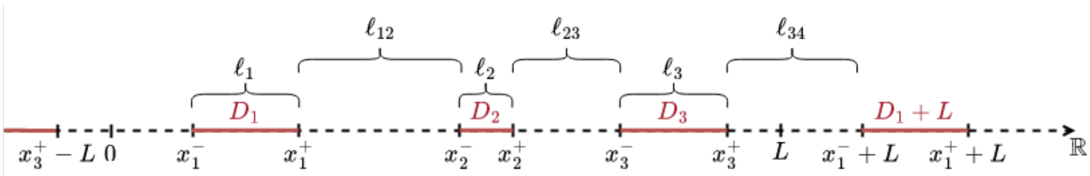

Figure 1: An illustration of the one-dimensional setting for $N = 3$ resonators in the unit cell.

In what follows, we denote by $Y := (0, L)$ the periodic unit cell and by

$$D := \bigsqcup_{i=1}^{N} (x_i^-, x_i^+) \tag{1}$$

the union of the N resonators in the unit cell. With this notation, the region within $\mathbb{R}$ which is taken up by the resonators, is given by

$$D + L\mathbb{Z} := \{x + kL \, : \, x \in D, \, k \in \mathbb{Z}\}. \tag{2}$$

2.2 Time-dependent material parameters

We assume that the material parameter distributions are periodic in x with period L and in t with period $T := 2\pi/\Omega$ and are given by

$$\kappa(x,t) = \begin{cases} \kappa_0, & x \notin D, \\ \kappa_\mathrm{r}\kappa_i(t), & x \in D_i, \end{cases} \qquad \rho(x,t) = \begin{cases} \rho_0, & x \notin D, \\ \rho_\mathrm{r}\rho_i(t), & x \in D_i. \end{cases} \tag{3}$$

Here, ρ and κ represent in acoustics the density and the bulk modulus of the material, respectively, and Ω is the frequency of the time-modulations of the material parameter distributions.

We define the contrast parameter and the wave speeds by

$$\delta := \frac{\rho_\mathrm{r}}{\rho_0}, \quad v_0 := \sqrt{\frac{\kappa_0}{\rho_0}}, \quad v_\mathrm{r} := \sqrt{\frac{\kappa_\mathrm{r}}{\rho_\mathrm{r}}}, \tag{4}$$

respectively. Typically, the most interesting regime of the frequency of modulations of $\rho_i(t)$ and $\kappa_i(t)$ is $\Omega = O(\delta^{1/2})$, *i.e.*, of the same order as the static subwavelength resonances [13]. This allows strong coupling between the time modulations and the response time of the structure.

We aim at finding $\omega = O(\delta^{1/2})$ such that the wave equation

$$\begin{cases} \left(\dfrac{1}{\kappa(x,t)}\dfrac{\partial^2}{\partial t^2} - \dfrac{\partial}{\partial x}\dfrac{1}{\rho(x,t)}\dfrac{\partial}{\partial x}\right) u(x,t) = 0, \quad x \in \mathbb{R},\, t \in \mathbb{R}, \\ u(x,t)\mathrm{e}^{-\mathrm{i}\omega t} \ \text{ is } T\text{−periodic}, \end{cases} \tag{5}$$

has a non-trivial solution $u(x,t)$ which is essentially supported in the *low-frequency regime.*

By substituting the time-harmonic wave field $u(x,t) = \Re\big(v(x,t)\mathrm{e}^{\mathrm{i}\omega t}\big)$ into the wave equation (5), we obtain

$$\frac{1}{\kappa(x,t)}\left(-\mathrm{i}\omega + \frac{\partial}{\partial t}\right)^2 v(x,t) - \frac{\partial}{\partial x}\left(\frac{1}{\rho(t,x)}\frac{\partial}{\partial x}v(x,t)\right) = 0, \quad x \in \mathbb{R},\, t \in \mathbb{R}. \tag{6}$$

Due to the assumption that $u(x,t)\mathrm{e}^{-\mathrm{i}\omega t}$ is T-periodic with respect to time t, we write the Fourier series expansion

$$u(x,t) = \mathrm{e}^{\mathrm{i}\omega t}\sum_{n=-\infty}^{\infty} v_n(x)\mathrm{e}^{\mathrm{i}n\Omega t}. \tag{7}$$

Note that any L^2-function $v_n(x)$ can be decomposed into a superposition of Bloch waves as follows:

$$v_n(x) = \int_{-\pi/L}^{\pi/L} \hat{v}_n(x,\alpha)\mathrm{e}^{\mathrm{i}\alpha x}\,\mathrm{d}\alpha, \tag{8}$$

where α is the so-called *momentum* and $\hat{v}_n(x,\alpha)$ is L-periodic in x. The function $\hat{v}_n$ is defined by

$$\hat{v}_n(x,\alpha) := \sum_{m=-\infty}^{\infty} v_n(x-mL)\mathrm{e}^{-\mathrm{i}\alpha(x-mL)}, \quad \forall\, n \in \mathbb{Z}. \tag{9}$$

Thus, we can write

$$u(x,t) = \mathrm{e}^{\mathrm{i}\omega t}\sum_{n=-\infty}^{\infty}\int_{-\pi/L}^{\pi/L} \hat{v}_n(x,\alpha)\mathrm{e}^{\mathrm{i}\alpha x}\,\mathrm{d}\alpha\,\mathrm{e}^{\mathrm{i}n\Omega t}. \tag{10}$$

Inserting the expansion (10) into the differential equation (6), we conclude that for any $n \in \mathbb{Z}$, $\hat{v}_n$ must satisfy

$$\begin{cases} -\dfrac{(\omega+n\Omega)^2}{\kappa(x,t)}\hat{v}_n - \left(\mathrm{i}\alpha + \dfrac{\partial}{\partial x}\right)\left(\dfrac{1}{\rho(x,t)}\left(\mathrm{i}\alpha + \dfrac{\partial}{\partial x}\right)\hat{v}_n\right) = 0, \quad x \in \mathbb{R},\, t \in \mathbb{R},\, \forall\, n \in \mathbb{Z}, \\ x \mapsto \hat{v}_n(x,\alpha) \text{ is } L\text{-periodic}. \end{cases} \tag{11}$$

Recall that we have assumed the chain of N resonators to be repeated periodically with period L. Therefore, we study the one-dimensional spectral problem in the unit cell $(0, L)$ for the quasiperiodic function $v_n(x,\alpha) := \hat{v}_n(x,\alpha)\mathrm{e}^{\mathrm{i}\alpha x}$:

$$\begin{cases} \left(\dfrac{\mathrm{d}^2}{\mathrm{d}x^2} + \dfrac{\rho_0(\omega+n\Omega)^2}{\kappa_0}\right) v_n = 0 & \text{in } (0,L) \setminus \bigsqcup_{i=1}^{N} \left(x_i^-, x_i^+\right), \\ \dfrac{\mathrm{d}^2}{\mathrm{d}x^2} v_{i,n}^* + \dfrac{\rho_\mathrm{r}(\omega+n\Omega)^2}{\kappa_\mathrm{r}} v_{i,n}^{**} = 0 & \text{in } \bigsqcup_{i=1}^{N} \left(x_i^-, x_i^+\right), \\ v_n|_-\left(x_i^\pm\right) = v_n|_+\left(x_i^\pm\right) & \text{for all } 1 \leq i \leq N, \\ \left.\dfrac{\mathrm{d}v_{i,n}^*}{\mathrm{d}x}\right|_+ \left(x_i^-\right) = \delta \left.\dfrac{\mathrm{d}v_n}{\mathrm{d}x}\right|_- \left(x_i^-\right) & \text{for all } 1 \leq i \leq N, \\ \left.\dfrac{\mathrm{d}v_{i,n}^*}{\mathrm{d}x}\right|_- \left(x_i^+\right) = \delta \left.\dfrac{\mathrm{d}v_n}{\mathrm{d}x}\right|_+ \left(x_i^+\right) & \text{for all } 1 \leq i \leq N, \end{cases} \tag{12}$$

where we use the notation

$$w|_\pm (x) := \lim_{s \to 0,\, s>0} w(x \pm s). \tag{13}$$

The functions $v_{i,n}^*(x,\alpha)$ and $v_{i,n}^{**}(x,\alpha)$ are defined in each resonator D_i through the convolutions

$$v_{i,n}^*(x,\alpha) = \sum_{m=-\infty}^{\infty} r_{i,m} v_{n-m}(x,\alpha), \quad v_{i,n}^{**}(x,\alpha) = \frac{1}{\omega+n\Omega} \sum_{m=-\infty}^{\infty} k_{i,m}(\omega+(n-m)\Omega) v_{n-m}(x,\alpha), \tag{14}$$

where $r_{i,m}$ and $k_{i,m}$ are the Fourier series coefficients of $1/\rho_i(t)$ and $1/\kappa_i(t)$. Furthermore, we define the wave number outside and inside the resonators corresponding to the n-th mode through

$$k^n := \frac{\omega+n\Omega}{v_0}, \quad k_\mathrm{r}^n := \frac{\omega+n\Omega}{v_\mathrm{r}}, \tag{15}$$

respectively. We assume that the time-modulations of ρ_i and κ_i have finite Fourier series in each resonator D_i, that is,

$$\frac{1}{\rho_i(t)} = \sum_{n=-M}^{M} r_{i,n} \mathrm{e}^{\mathrm{i}n\Omega t}, \quad \frac{1}{\kappa_i(t)} = \sum_{n=-M}^{M} k_{i,n} \mathrm{e}^{\mathrm{i}n\Omega t} \tag{16}$$

for some $M \in \mathbb{N}$ satisfying $M = O\left(\delta^{-\gamma/2}\right)$, for some $\gamma \in (0,1)$ [13]. Note that the solution to (12) is invariant under scaling. Hence, we can assume the solution to be normalized. As u is continuously differentiable in t, we have

$$\|v_n\|_2 = o\left(\frac{1}{n}\right) \quad \text{as } n \to \infty, \tag{17}$$

where $\|\cdot\|_2$ denotes the L^2-norm on $(0, L)$. Due to folding (see Definition 5.1), we need to specify the subwavelength quasifrequencies in terms of the oscillations in their associated modes [13]. As said before, the subwavelength quasifrequencies are those associated with Bloch modes essentially supported in the low-frequency regime as $\delta \to 0$. Therefore, we shall assume that there exists some $M_v = M_v(\delta) \in \mathbb{N}$ such that

$$M_v\Omega \to 0 \quad \text{and} \quad \sum_{n=-\infty}^{\infty} ||v_n||_2 = \sum_{n=-M_v}^{M_v} ||v_n||_2 + o(1), \tag{18}$$

as $\delta \to 0$, where the sequence of functions $(v_n)_{n\in\mathbb{Z}}$ is a nontrivial solution to (12). As we will see later, we can assume without loss of accuracy that $M_v = M$.

In order to perform some numerical and analytic analysis in this regime, we adapt the Dirichlet-to-Neumann approach of [21, 22] to the one-dimensional, quasi-periodic and time-modulated case to solve (12).

3 Exact solution

In this section we seek to solve the modified Helmholtz problem (12) exactly. We first present a characterization of the solution to the exterior problem and then to the interior problem. Lastly, we use the Dirichlet-to-Neumann map to derive a system of equations based on the boundary condition.

3.1 Exterior problem

In this section we seek to characterize the Dirichlet-to-Neumann map of the Helmholtz operator on the domain $(0, L)$ with the quasi-periodic boundary condition.

We denote the Sobolev space of quasiperiodic complex-valued functions by $H^1_{\mathrm{per},\alpha}(\mathbb{R})$. We also denote by $\mathbb{C}^{2N,\alpha}$ the set of quasi-periodic boundary data $f \equiv (f_i^{\pm})_{i\in\mathbb{Z}}$ such that

$$f_{i+N}^{\pm} = \mathrm{e}^{\mathrm{i}\alpha L} f_i^{\pm}, \tag{19}$$

where f_i^+ (resp. f_i^-) refers to the component associated with x_i^+ (resp. with x_i^-). The space of such quasi-periodic sequences is clearly finite-dimensional, specifically it is of dimension $2N$.

The following lemma from [22] provides an explicit expression for the solution to the exterior problem on $\mathbb{R} \setminus (D + L\mathbb{Z})$.

Lemma 3.1. *Assume that $k^n = (\omega + n\Omega)/v_0$, for some fixed $n \in \mathbb{Z}$, is not of the form $m\pi/\ell_{i(i+1)}$ for some non-zero integer $m \in \mathbb{Z}\backslash\{0\}$ and index $1 \le i \le N$. Then, for any quasi-periodic sequence $(f_i^{\pm})_{1\le i\le N} \in \mathbb{C}^{2N,\alpha}$, there exists a unique solution $v_{f,n}^{\alpha} \in H^1_{\mathrm{per},\alpha}(\mathbb{R})$ to the exterior problem:*

$$\begin{cases} \left(\dfrac{\mathrm{d}^2}{\mathrm{d}x^2} + (k^n)^2\right) v_{f,n}^{\alpha} = 0 & \text{in } \mathbb{R}\backslash(D + L\mathbb{Z}), \\ v_{f,n}^{\alpha}(x_i^{\pm}) = f_i^{\pm} & \text{for all } 1 \le i \le N, \\ v_{f,n}^{\alpha}(x + L) = \mathrm{e}^{\mathrm{i}\alpha L} v_{f,n}^{\alpha}(x) & \text{in } \mathbb{R} \setminus (D + L\mathbb{Z}). \end{cases} \tag{20}$$

Furthermore, when $k^n \neq 0$, the solution $v_{f,n}^{\alpha}$ reads explicitly

$$v_{f,n}^{\alpha}(x) = \alpha_i^n \mathrm{e}^{\mathrm{i}k^n x} + \beta_i^n \mathrm{e}^{-\mathrm{i}k^n x} \text{ if } x \in (x_i^+, x_{i+1}^-), \qquad \forall i \in \mathbb{Z}, \tag{21}$$

where, for fixed $n \in \mathbb{Z}$, α_i^n and β_i^n are given by the matrix-vector product

$$\begin{bmatrix} \alpha_i^n \\ \beta_i^n \end{bmatrix} = -\frac{1}{2\mathrm{i}\sin(k^n \ell_{i(i+1)})} \begin{bmatrix} \mathrm{e}^{-\mathrm{i}k^n x_{i+1}^-} & -\mathrm{e}^{-\mathrm{i}k^n x_i^+} \\ -\mathrm{e}^{\mathrm{i}k^n x_{i+1}^-} & \mathrm{e}^{\mathrm{i}k^n x_i^+} \end{bmatrix} \begin{bmatrix} f_i^+ \\ f_{i+1}^- \end{bmatrix}. \tag{22}$$

Proof. Identical to [22, Lemma 2.1]. □

Definition 3.1. For any $k^n \in \mathbb{C}$, for fixed $n \in \mathbb{Z}$, which is not of the form $m\pi/\ell_{i(i+1)}$ for some $m \in \mathbb{Z}\backslash\{0\}$ and $1 \leq i \leq N-1$, the *Dirichlet-to-Neumann map* with wave number k^n is the linear operator $\mathcal{T}^{k^n,\alpha} : \mathbb{C}^{2N,\alpha} \to \mathbb{C}^{2N,\alpha}$ defined by

$$\mathcal{T}^{k^n,\alpha}[(f_i^{\pm})_{1\leq i\leq N}] := \left(\pm \frac{\mathrm{d}v_{f,n}^{\alpha}}{\mathrm{d}x}(x_i^{\pm}) \right)_{1\leq i\leq N}, \tag{23}$$

where $v_{f,n}^{\alpha}$ is the unique solution to (20).

Using the exponential Ansatz presented in Lemma 3.1 to solve (20) gives rise to a closed form definition of the Dirichlet-to-Neumann map, which we introduce in the following proposition.

Proposition 3.2. *For fixed $n \in \mathbb{Z}$, the Dirichlet-to-Neumann map $\mathcal{T}^{k^n,\alpha}$ admits the following explicit matrix representation: for any $k^n \in \mathbb{C}\backslash\{m\pi/\ell_{i(i+1)} : m \in \mathbb{Z}\backslash\{0\}, 1 \leq i \leq N-1\}$, $f \equiv (f_i^{\pm})_{1\leq i\leq N}$, $\mathcal{T}^{k^n,\alpha}[f] \equiv (\mathcal{T}^{k^n,\alpha}[f]_i^{\pm})_{1\leq i\leq N}$ is given by*

$$\begin{bmatrix} \mathcal{T}^{k^n,\alpha}[f]_1^- \\ \mathcal{T}^{k^n,\alpha}[f]_1^+ \\ \vdots \\ \mathcal{T}^{k^n,\alpha}[f]_N^- \\ \mathcal{T}^{k^n,\alpha}[f]_N^+ \end{bmatrix} = \begin{bmatrix} -\frac{k^n\cos(k^n\ell_{N(N+1)})}{\sin(k^n\ell_{N(N+1)})} & & & & & \frac{k^n}{\sin(k^n\ell_{N(N+1)})}\mathrm{e}^{-\mathrm{i}\alpha L} \\ & A^{k^n}(\ell_{12}) & & & & \\ & & A^{k^n}(\ell_{23}) & & & \\ & & & \ddots & & \\ & & & & A^{k^n}(\ell_{(N-1)N}) & \\ \frac{k^n}{\sin(k^n\ell_{N(N+1)})}\mathrm{e}^{\mathrm{i}\alpha L} & & & & & -\frac{k^n\cos(k^n\ell_{N(N+1)})}{\sin(k^n\ell_{N(N+1)})} \end{bmatrix} \begin{bmatrix} f_1^- \\ f_1^+ \\ \vdots \\ f_N^- \\ f_N^+ \end{bmatrix}, \tag{24}$$

where for any $\ell \in \mathbb{R}$, $A^{k^n}(\ell)$ denotes the 2×2 symmetric matrix

$$A^{k^n}(\ell) := \begin{bmatrix} -\frac{k^n\cos(k^n\ell)}{\sin(k^n\ell)} & \frac{k^n}{\sin(k^n\ell)} \\ \frac{k^n}{\sin(k^n\ell)} & -\frac{k^n\cos(k^n\ell)}{\sin(k^n\ell)} \end{bmatrix}. \tag{25}$$

Proof. Identical to [1, Proposition 3.3]. □

To this end, we have found a way to solve the exterior problem explicitly for some given boundary data, as stated in Lemma 3.1. Moreover, we have proved an explicit matrix representation of the Dirichlet-to-Neumann map in Proposition 3.2, which we will make use of when dealing with the Neumann boundary condition of (12) in order to solve the interior problem.

3.2 Interior problem

Having dealt with the exterior problem in the previous section, we now focus on the solution of the interior problem. We can formulate the interior part of problem (12) using the Dirichlet-to-Neumann map, which leads to

$$\begin{cases} \frac{\mathrm{d}^2}{\mathrm{d}x^2}v_{i,n}^* + \frac{\rho_\mathrm{r}(\omega+n\Omega)^2}{\kappa_\mathrm{r}}v_{i,n}^{**} = 0 & \text{in } D + L\mathbb{Z}, \\ \pm\frac{\mathrm{d}}{\mathrm{d}x}v_n^*(x_i^{\pm},\alpha) = \delta\mathcal{T}^{k^n,\alpha}[v_n]_i^{\pm} & \text{for all } i \in \mathbb{Z}, \\ v_n(x+L,\alpha) = \mathrm{e}^{\mathrm{i}\alpha L}v_n(x,\alpha) & \text{for almost every } x \in D + L\mathbb{Z}, \end{cases} \tag{26}$$

for $n \in \mathbb{Z}$. Recall that $v^{*}_{i,n}$ and $v^{**}_{i,n}$ are the convolutions defined by (14).

We now recall the definition of a subwavelength quasifrequency [13].

Definition 3.2. Any frequency $\omega^\alpha(\delta) \in [-\Omega/2, \Omega/2)$ for which the v_n's satisfying (26) are not all trivial and the corresponding

$$u^\alpha(x,t) = \mathrm{e}^{\mathrm{i}\omega^\alpha(\delta)t} \sum_{n=-\infty}^{\infty} v_n(x,\alpha)\mathrm{e}^{\mathrm{i}n\Omega t} \tag{27}$$

is essentially supported in the low-frequency regime, *i.e.*, there exists M_v such that (18) holds, is called a *subwavelength quasifrequency.* Moreover, u^α is called a *subwavelength Bloch mode* associated to $\omega^\alpha(\delta)$.

Next, we state the following lemma, which provides us with the solution to the interior problem upon using an exponential Ansatz. The idea behind this lemma is taken from [1] and adapted to the time-modulated setting considered in this paper.

Lemma 3.3. *The subwavelength quasifrequencies ω to the wave problem (26) are approximately satisfying as δ goes to zero the following truncated $2N \times 2N$ coupled system of non-linear equations:*

$$\sum_{m=-M_v}^{M_v} r_{i,m}\mathcal{G}^{n-m}(\omega)\begin{bmatrix} a_i^{n-m} \\ b_i^{n-m}\end{bmatrix}_{1\leq i\leq N} - \delta\mathcal{T}^{k^n,\alpha} \times \mathcal{V}^n(\omega)\begin{bmatrix} a_i^{n} \\ b_i^{n}\end{bmatrix}_{1\leq i\leq N} = 0, \quad \forall -M_v \leq n \leq M_v, \tag{28}$$

for some $M_v \in \mathbb{N}$ such that $M_v\Omega \to 0$ as $\delta \to 0$ and a non-trivial $(a_i^n, b_i^n)_{1\leq i\leq N, |n|\leq M_v}$. Here, $\mathcal{T}^{k^n,\alpha}$ denotes the Dirichlet-to-Neumann map, which is a $2N \times 2N$ matrix defined by (24) and we have used the following notation:

$$\mathcal{G}^{n-m}(\omega) := \mathrm{diag}\left(\mathcal{G}_i^{n,m}(\omega)\right)_{1\leq i\leq N}, \qquad \mathcal{V}^{n-m}(\omega) := \mathrm{diag}\left(\mathcal{V}_i^{n,m}(\omega)\right)_{1\leq i\leq N}, \tag{29}$$

$$\mathcal{G}_i^{n,m}(\omega) := \mathrm{i}k_\mathrm{r}^n\gamma_i^{(n,m)}\begin{bmatrix} -\mathrm{e}^{\mathrm{i}k_\mathrm{r}^n\gamma_i^{(n,m)}x_i^-} & \mathrm{e}^{-\mathrm{i}k_\mathrm{r}^n\gamma_i^{(n,m)}x_i^-} \\ \mathrm{e}^{\mathrm{i}k_\mathrm{r}^n\gamma_i^{(n,m)}x_i^+} & -\mathrm{e}^{-\mathrm{i}k_\mathrm{r}^n\gamma_i^{(n,m)}x_i^+}\end{bmatrix}, \quad \mathcal{V}_i^{n,m}(\omega) := \begin{bmatrix} \mathrm{e}^{\mathrm{i}k_\mathrm{r}^n\gamma_i^{(n,m)}x_i^-} & \mathrm{e}^{-\mathrm{i}k_\mathrm{r}^n\gamma_i^{(n,m)}x_i^-} \\ \mathrm{e}^{\mathrm{i}k_\mathrm{r}^n\gamma_i^{(n,m)}x_i^+} & \mathrm{e}^{-\mathrm{i}k_\mathrm{r}^n\gamma_i^{(n,m)}x_i^+}\end{bmatrix}, \tag{30}$$

where

$$\gamma_i^{(n,m)} := \sqrt{\frac{\omega+(n-m)\Omega}{\omega+n\Omega}\frac{k_{i,m}}{r_{i,m}}}. \tag{31}$$

Furthermore, the subwavelength Bloch modes to (26) correspond approximately to the solution $\begin{bmatrix} a_i^n & b_i^n\end{bmatrix}^T_{1\leq i\leq N}$, where the superscript T denotes the transpose, through the formula

$$v_{n-m}(x) = a_i^{n-m}\mathrm{e}^{\mathrm{i}k_r^n\gamma_i^{(n,m)}x} + b_i^{n-m}\mathrm{e}^{-\mathrm{i}k_r^n\gamma_i^{(n,m)}x}, \quad \forall\, x \in \left(x_i^-, x_i^+\right), \tag{32}$$

and $a_i^n = b_i^n = 0$ for all $1 \leq i \leq N$ and $|n| > M_v$. This allows us to introduce a $2N(2M_v+1) \times 2N(2M_v+1)$ matrix $\mathcal{A}^*(\omega,\delta)$, which is such that we can define the following system of equations:

$$\mathcal{A}^*(\omega,\delta)\mathbf{w} = \mathbf{0}, \quad \mathbf{w} := \begin{bmatrix} \mathbf{v}_{-M_v} \\ \vdots \\ \mathbf{v}_0 \\ \vdots \\ \mathbf{v}_{M_v}\end{bmatrix}, \quad \mathbf{v}_n := \begin{bmatrix} a_i^n \\ b_i^n \end{bmatrix}_{1\leq i\leq N}. \tag{33}$$

Then, for given δ small enough, the subwavelength quasifrequencies are approximately the characteristic values of $\mathcal{A}^*(\omega, \delta)$.

We present the proof to a more specific formulation of Lemma 3.3 in Section 3.3.

Remark 3.3. For fixed N, the size of the matrix $\mathcal{A}^*$ depends solely on the number M_v of dominant Fourier modes v_n in the Fourier series of v. The number of non-zero off-diagonals in the matrix $\mathcal{A}^*$ depends on the number M of considered Fourier coefficients of $1/\rho_i(t)$ and $1/\kappa_i(t)$. Hence, we can choose the number of non-zero modes v_n to be exactly the same as the number of Fourier coefficients of $1/\rho_i(t)$ and $1/\kappa_i(t)$. We have numerically checked that taking M_v higher than M does not change the values of the subwavelength quasifrequencies for δ small enough. Figure 2a shows that for increasing M_v, the time it takes to solve (33) for ω increases. Moreover, Figure 2b confirms that the resulting error between the value of ω obtained through Lemma 3.3 and through the capacitance matrix approximation, as discussed in Section 5.1, does not depend on M_v. Therefore, the earlier stated assumption $M_v = M$ is accurate for δ small enough.

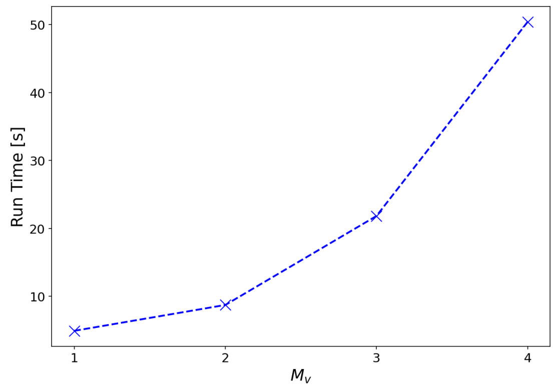

(a) The time it takes to solve (33) for ω depending on the value of M_v, while the other parameters stay fixed. The run time increases with increasing M_v.

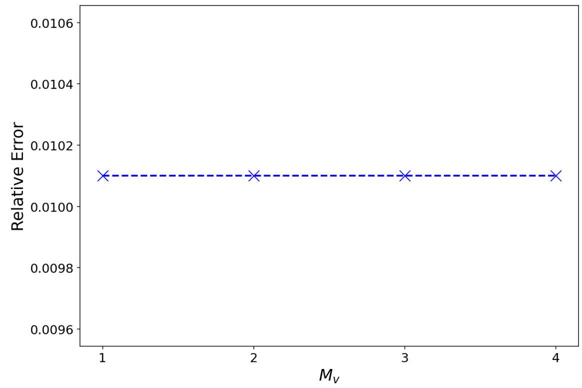

(b) The relative error between the approximate solution based on the capacitance approximation, as introduced in Section 5.1, and the ω obtained through solving (33).

Figure 2: For $M = 1$ with fixed values for N, $r_{i,m}$, $k_{i,m}$, δ, Ω, we increase M_v and measure the run time and resulting relative error.

3.3 Explicit choice of M

We now assume that ρ_i and κ_i are specifically given by

$$\rho_i(t) := \frac{1}{1 + \varepsilon_{\rho,i}\cos(\Omega t + \phi_{\rho,i})}, \quad \kappa_i(t) := \frac{1}{1 + \varepsilon_{\kappa,i}\cos(\Omega t + \phi_{\kappa,i})}, \tag{34}$$

for all $1 \le i \le N$, where $\varepsilon_{\rho,i}$, $\varepsilon_{\kappa,i}$ are the amplitudes of the time-modulations and $\phi_{\rho,i}$, $\phi_{\kappa,i}$ the phase shifts. This means that we can set $M = 1$ with the Fourier coefficients defined as follows:

$$r_{i,-1} := \frac{\varepsilon_{\rho,i}\mathrm{e}^{-\mathrm{i}\phi_{\rho,i}}}{2}, \quad r_{i,0} := 1, \quad r_{i,1} := \frac{\varepsilon_{\rho,i}\mathrm{e}^{\mathrm{i}\phi_{\rho,i}}}{2}, \tag{35}$$

$$k_{i,-1} := \frac{\varepsilon_{\kappa,i}\mathrm{e}^{-\mathrm{i}\phi_{\kappa,i}}}{2}, \quad k_{i,0} := 1, \quad k_{i,1} := \frac{\varepsilon_{\kappa,i}\mathrm{e}^{\mathrm{i}\phi_{\kappa,i}}}{2}. \tag{36}$$

Having an explicit definition of the material parameters ρ and κ we now want to reformulate Lemma 3.3 such that it corresponds to $\rho_i(t)$ and $\kappa_i(t)$ defined by (34).

Lemma 3.4. *If $M_v = M = 1$, then (28) reduces to the following $2N \times 2N$ coupled systems of non-linear equations:*

$$
\begin{aligned}
r_{i,-1}\mathcal{G}^{n+1}(\omega)\begin{bmatrix} a_i^{n+1} \\ b_i^{n+1} \end{bmatrix}_{1\leq i\leq N} &+ r_{i,0}\mathcal{G}^{n}(\omega)\begin{bmatrix} a_i^{n} \\ b_i^{n} \end{bmatrix}_{1\leq i\leq N} + r_{i,1}\mathcal{G}^{n-1}(\omega)\begin{bmatrix} a_i^{n-1} \\ b_i^{n-1} \end{bmatrix}_{1\leq i\leq N} \\
&= \delta\mathcal{T}^{k^n,\alpha} \times \mathcal{V}^n(\omega)\begin{bmatrix} a_i^{n} \\ b_i^{n} \end{bmatrix}_{1\leq i\leq N},
\end{aligned}
\tag{37}
$$

for $-1 \leq n \leq 1$, where the matrices $\mathcal{G}^{n-m}(\omega)$ and $\mathcal{V}^{n-m}(\omega)$ are defined by (29). Moreover, $\mathcal{A}^*(\omega,\delta)$ is the $6N \times 6N$ matrix given by

$$
\mathcal{A}^*(\omega,\delta) := \begin{bmatrix} \mathcal{A}^{-1}(\omega,\delta) \\ \mathcal{A}^{0}(\omega,\delta) \\ \mathcal{A}^{1}(\omega,\delta) \end{bmatrix},
\tag{38}
$$

where the matrices $\mathcal{A}^{-1}$, $\mathcal{A}^0$, and $\mathcal{A}^1$ are defined by

$$
\mathcal{A}^{-1}(\omega,\delta) := \begin{bmatrix} \left(\mathbf{r}_0\mathcal{G}^{-1-0}(\omega) - \delta\mathcal{T}^{k^{-1},\alpha}\mathcal{V}^{-1-0}\right) & \mathbf{r}_{-1}\mathcal{G}^{-1+1} & 0 \end{bmatrix},
\tag{39}
$$

$$
\mathcal{A}^{0}(\omega,\delta) := \begin{bmatrix} \mathbf{r}_1\mathcal{G}^{0-1}(\omega) & \left(\mathbf{r}_0\mathcal{G}^{0-0}(\omega) - \delta\mathcal{T}^{k^{0},\alpha}\mathcal{V}^{0-0}(\omega)\right) & \mathbf{r}_{-1}\mathcal{G}^{0+1}(\omega) \end{bmatrix},
\tag{40}
$$

$$
\mathcal{A}^{1}(\omega,\delta) := \begin{bmatrix} 0 & \mathbf{r}_1\mathcal{G}^{1-1}(\omega) & \left(\mathbf{r}_0\mathcal{G}^{1-0}(\omega) - \delta\mathcal{T}^{k^{1},\alpha}\mathcal{V}^{1-0}(\omega)\right) \end{bmatrix},
\tag{41}
$$

with $\mathbf{r}_n := (r_{i,n})_{1\leq i\leq N}$ being the vector of the n-th Fourier coefficients in each resonator. Consequently, we obtain the following system of equations:

$$
\mathcal{A}^*(\omega,\delta)\mathbf{w} = \mathbf{0}, \quad \mathbf{w} := \begin{bmatrix} \mathbf{v}_{-1} \\ \mathbf{v}_0 \\ \mathbf{v}_1 \end{bmatrix}, \quad \mathbf{v}_n := \begin{bmatrix} a_i^{n} \\ b_i^{n} \end{bmatrix}_{1\leq i\leq N}.
\tag{42}
$$

Proof. Any solution v_n to (26) can be written as (32), and the boundary condition of (26) reads, for all $1 \leq i \leq N$

$$
\begin{aligned}
\pm\mathrm{i}\sum_{m=-1}^{1} r_{i,m}k_{\mathrm{r}}^{n-m}\left(a_i^{n-m}\mathrm{e}^{\mathrm{i}\gamma_i^{(n,m)}k_{\mathrm{r}}^{n-m}x_i^{\pm}} - b_i^{n-m}\mathrm{e}^{-\mathrm{i}\gamma_i^{(n,m)}k_{\mathrm{r}}^{n-m}x_i^{\pm}}\right) - \delta\mathcal{T}^{k^n,\alpha}[a_i^n\mathrm{e}^{\mathrm{i}\gamma_i^{(n,m)}k_{\mathrm{r}}^{n}x} \\
+ b_i^n\mathrm{e}^{-\mathrm{i}\gamma_i^{(n,m)}k_{\mathrm{r}}^{n}x}]_i^{\pm} = 0,
\end{aligned}
$$

which can be written as (42) by evaluating it for $n = -1, 0, 1$. □

Remark 3.4. We have now found a characterization of the subwavelength quasifrequencies $\omega^\alpha(\delta)$ through the solution of the interior problem, as stated in Lemma 3.4. The definition (38) of the matrix $\mathcal{A}^*(\omega,\delta)$ was done for a specific choice of $\rho_i(t)$ and $\kappa_i(t)$, and hence, also M. However, the matrix $\mathcal{A}^*(\omega,\delta)$ can equivalently be defined for any choice of material parameters and M.

4 Muller's method

We solve problem (12) with the help of Muller's method. In particular, we use Lemma 3.3 to construct a $2N(2M+1) \times 2N(2M+1)$ system of equations $\mathcal{A}^*(\omega,\delta)\mathbf{w} = \mathbf{0}$, which provides the correct coefficients a_i^n and b_i^n of the n-th mode v_n in each resonator D_i. We seek to find the subwavelength quasifrequencies $\omega^\alpha(\delta)$, which are those values of ω for which the interior problem (26) admits a non-trivial solution. Note that these are exactly the values of ω for which $\mathcal{A}^*(\omega,\delta)$ is non-invertible, *i.e.*, $\det(\mathcal{A}^*(\omega,\delta)) = 0$. Therefore, we define the function $f(\omega) := \det(\mathcal{A}^*(\omega,\delta))$ whose zeros we must find, for a fixed δ. In order to find the zeros of the non-linear function $f(\omega)$, we use Muller's method upon three initial guesses per root. For a detailed explanation of Muller's method we refer the reader to [10, Section 1.6]. One of the reasons for using Muller's method to solve the root-finding problem is that, unlike other root-finding algorithms, Muller's method is well-suited for complex-valued problems [10, Section 1.6].

Muller's method requires the definition of three initial guesses to find a zero of $f(\omega)$. In our numerical computations we make use of the already known definition of the capacitance matrix C^α_{static} in the static case [1], as further explained in Appendix A. Namely, we compute the eigenvalues λ_i^α, $1 \le i \le N$, of the static generalized capacitance matrix $\mathcal{C}^\alpha_{\text{static}}$ and employ the asymptotic approximation from [22]

$$\omega_i^\alpha \approx \pm v_{\mathrm{r}} \sqrt{\lambda_i^\alpha \delta}, \quad \forall\, 1 \le i \le N. \tag{43}$$

To initialize Muller's method we use (43) and two perturbations of this value.

By the definition of Muller's method we need to supply the algorithm with three initial guesses in order to find a zero of $f(\omega)$, which is not trivial. Furthermore, the run time of Muller's method grows exponentially in N, as illustrated in Figure 3b. Therefore, we seek to introduce an alternative characterization of the subwavelength quasifrequencies ω^α, for which we do not require the exact solution of (26). In view of this, we introduce a discrete approximation of (12) in Section 5.1.

5 Capacitance approximation and asymptotic analysis

5.1 Capacitance matrix formulation

By fixing an $\alpha \in Y^* := (-\pi/L, \pi/L]$, we seek subwavelength quasifrequencies ω of (12). Following the proof of Lemma 4.1 outlined in [13], we can obtain the following result.

Lemma 5.1. *As $\delta \to 0$, the functions $v^*_{i,n}(x,\alpha)$ are approximately constant inside the resonator:*

$$v^*_{i,n}(x,\alpha)\big|_{(x_j^-,x_j^+)} = c_{j,n} + O(\delta^{(1-\gamma)/2}). \tag{44}$$

For simplicity of notation, we define for any smooth function $f : \mathbb{R} \to \mathbb{R}$ the following:

$$I_{\partial D_j}(f) := \left.\frac{\mathrm{d}f}{\mathrm{d}x}\right|_-(x_j^-) - \left.\frac{\mathrm{d}f}{\mathrm{d}x}\right|_+(x_j^+). \tag{45}$$

In view of this notation, we observe that

$$I_{\partial D_i}(v^*_{i,n}) = I_{\partial D_i}\left(\sum_{j=1}^N c_{j,n} V_j^\alpha\right) = \sum_{j=1}^N c_{j,n} C_{ij}^\alpha, \tag{46}$$

where V_j^α and the capacitance matrix coefficients C_{ij}^α are defined as in the static case [1]; see Appendix A. On the other hand, we can insert the transmission conditions in (12) to obtain

$$\begin{aligned} I_{\partial D_i}(v_n) &= \frac{1}{\delta}\left(\left.\frac{\mathrm{d}v^*_{i,n}}{\mathrm{d}x}\right|_+(x_i^-,\alpha) - \left.\frac{\mathrm{d}v^*_{i,n}}{\mathrm{d}x}\right|_-(x_i^+,\alpha)\right) \\ &= -\frac{1}{\delta}\int_{x_i^-}^{x_i^+} \frac{\mathrm{d}^2 v^*_{i,n}}{\mathrm{d}x^2}(x,\alpha)\,\mathrm{d}x \\ &= \frac{1}{\delta}\int_{x_i^-}^{x_i^+} \frac{\rho_{\mathrm{r}}(\omega+n\Omega)^2}{\kappa_{\mathrm{r}}} v^{**}_{i,n}(x,\alpha)\,\mathrm{d}x. \end{aligned} \tag{47}$$

Therefore, $I_{\partial D_i}(v_{i,n}^*(x,\alpha))$ reads

$$I_{\partial D_i}(v_{i,n}^*) = \frac{\rho_\mathrm{r}}{\delta \kappa_\mathrm{r}} \sum_{m=-M}^{M} r_{i,m}(\omega + (n-m)\Omega)^2 \int_{x_i^-}^{x_i^+} v_{i,n-m}^{**}(x,\alpha)\,\mathrm{d}x. \tag{48}$$

Equating (46) and (48) yields

$$\sum_{j=1}^{N} c_{j,n} C_{ij}^\alpha = \frac{\rho_\mathrm{r}}{\delta \kappa_\mathrm{r}} \sum_{m=-M}^{M} r_{i,m}(\omega + (n-m)\Omega)^2 \int_{x_i^-}^{x_i^+} v_{i,n-m}^{**}(x,\alpha)\,\mathrm{d}x + O\left(\delta^{(1-\gamma)/2}\right). \tag{49}$$

Following the same argument laid out in [13] and using the same notation, we arrive at the following result.

Theorem 5.2. *Assuming the material parameters are given by (3), as $\delta \to 0$, the quasifrequencies in the subwavelength regime are, at leading order, given by the quasifrequencies of the ordinary differential equation:*

$$M^\alpha(t)\Psi(t) + \Psi''(t) = 0, \tag{50}$$

where $M^\alpha(t) = \frac{\delta\kappa_\mathrm{r}}{\rho_\mathrm{r}} W_1(t) C^\alpha W_2(t) + W_3(t)$ with W_1, W_2 and W_3 being diagonal matrices defined as

$$(W_1)_{ii} = \frac{\sqrt{\kappa_i}\rho_i}{|D_i|}, \qquad (W_2)_{ii} = \frac{\sqrt{\kappa_i}}{\rho_i}, \qquad (W_1)_{ii} = \frac{\sqrt{\kappa_i}}{2}\frac{\mathrm{d}}{\mathrm{d}t}\frac{\kappa_i'}{\kappa_i^{3/2}}, \tag{51}$$

for $i = 1, \dots, N$.

Our numerical results presented in Figure 3 corroborate our analytically proven claim that the capacitance matrix approximation is an efficient and effective alternative to the exact computation of the subwavelength quasifrequencies using Muller's method.

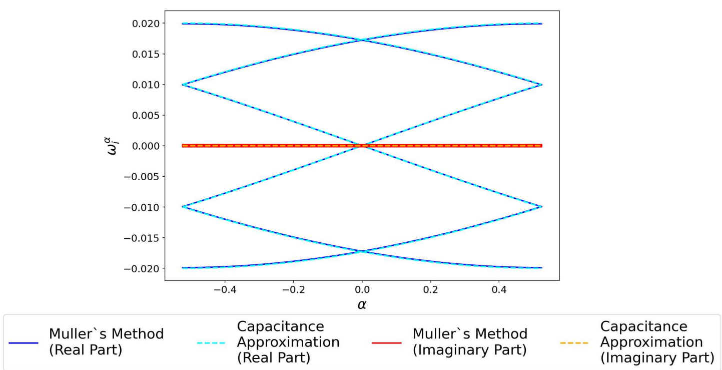

(a) The relative error corresponding to this result is given by $err_\mathrm{rel} = 0.0101$.

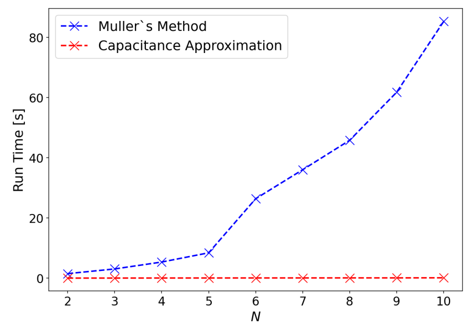

(b) We compare the time it takes Muller's method to solve the root-finding problem with the time it takes the capacitance approximation to solve the problem.

Figure 3: Comparing the results obtained with Muller's method and the capacitance matrix approximation for $\delta = 0.0001$, $\Omega = 0.05$, $\varepsilon_\rho = \varepsilon_\kappa = 0$, $v_0 = 1$, $v_\mathrm{r} = 1$, $\phi_{\rho,i} = \phi_{\kappa,i} = \pi/i$, with each resonator being of length $\ell_i = 1$ with equal spacing $\ell_{ij} = 1$.

To compare the results obtained by Muller's method $\omega_{i,\mathrm{muller}}^\alpha$ and the capacitance approximation $\omega_{i,\mathrm{cap}}^\alpha$, we consider the relative error defined by

$$err_\mathrm{rel} := \max_{\alpha\in[-\pi/L,\pi/L]} \max_{i=1,\dots,N} \frac{||\omega_{i,\mathrm{muller}}^\alpha - \omega_{i,\mathrm{cap}}^\alpha||_\mathbb{C}}{||\omega_{i,\mathrm{muller}}^\alpha||_\mathbb{C}}, \tag{52}$$

where $\|\cdot\|_{\mathbb{C}}$ denotes the complex euclidean norm. Closer investigations on the obtained error revealed that if $\Im(\omega_i^\alpha) = 0$, Muller's method is unable to exactly recover this. Thus, the error between $\Im(\omega_{i,\text{muller}}^\alpha)$ and $\Im(\omega_{i,\text{cap}}^\alpha)$ may be higher than expected. However, this is due to the fact that Muller's method is unable to exactly determine a non-zero purely real root.

5.2 Asymptotic analysis

To conduct some asymptotic analysis, we assume the modulation amplitudes of ρ_i and κ_i to be the same over all resonators, *i.e.*, $\varepsilon_{\rho,i} = \varepsilon_{\kappa,i} = \varepsilon$, for all $1 \leq i \leq N$. To analyze the reciprocity properties of the wave transmission we make use of asymptotic Floquet analysis developed in [12] and we closely follow [4]. Firstly, assume that the matrix $M^\alpha(t)$ in (50) is analytic in ε, whence, we can expand $M^\alpha(t)$ as follows [4]:

$$M^\alpha(t) = M_0^\alpha + \varepsilon M_1^\alpha(t) + \cdots + \varepsilon^n M_n^\alpha(t) + \ldots, \tag{53}$$

for small $\varepsilon > 0$. If $\rho_i(t)$ and $\kappa_i(t)$ have finitely many Fourier coefficients, we can assume that the series (53) converges for any $|\varepsilon| < \varepsilon_0$, for some $\varepsilon_0 > 0$ [3, 12]. Note that we omit the superscript α in the remainder of this section for the sake of convenience. Next, we rewrite the second order ODE (50) into the first order ODE [4]

$$\frac{\mathrm{d}\mathbf{y}}{\mathrm{d}t}(t) = A(t)\mathbf{y}(t), \quad A(t) := \begin{bmatrix} 0 & \mathrm{Id}_N \\ -M(t) & 0 \end{bmatrix}, \tag{54}$$

where Id_N is the $N \times N$ identity matrix. By Floquet's theorem, the fundamental solution of (54) can be written as $X(t) = P(t)\mathrm{e}^{Ft}$, for some matrices $P(t)$ and F [37]. As a consequence of $M(t)$ being analytic in ε, we can write [4]

$$\begin{cases} A(t) = A_0 + \varepsilon A_1(t) + \cdots + \varepsilon^n A_n(t) + \ldots, \\ P(t) = P_0 + \varepsilon P_1(t) + \cdots + \varepsilon^n P_n(t) + \ldots, \\ F = F_0 + \varepsilon F_1 + \cdots + \varepsilon^n F_n + \ldots. \end{cases} \tag{55}$$

The coefficients A_0 and P_0 are not time-dependent, as they correspond to $\varepsilon = 0$, which represents exactly the static case. Due to the T-periodicity of the material parameters, $A(t)$ is T-periodic and, thus, $A_j(t)$ are also T-periodic, for all $j \geq 1$. Hence, we may write [4]

$$A_j(t) = \sum_{m=-\infty}^{\infty} A_j^{(m)} \mathrm{e}^{\mathrm{i}\Omega m t}. \tag{56}$$

We now aim to derive asymptotic expansions of the eigenvalues $f = f_0 + \varepsilon f + \ldots$ of F in ε. Assume the first coefficient A_0 in the expansion of $A(t)$ to be diagonal. Then, according to [4], we have

$$F_0 = A_0 - \mathrm{i}\Omega \begin{bmatrix} m_1 & & \\ & \ddots & \\ & & m_n \end{bmatrix} \tag{57}$$

with m_i being the folding number of $(A_0)_{ii}$, which is defined as follows.

Definition 5.1. Let ω_{A_0} be the imaginary part of an eigenvalue of the matrix A_0. Then, we can uniquely write $\omega_{A_0} = \omega_0 + m\Omega$, where $\omega_0 \in [-\Omega/2, \Omega/2)$. The integer m is called the *folding number* [4].

We are specifically interested in investigating perturbations due to the modulations at a degenerate point f_0 of F_0, which can be obtained through folding, for which we make use of the following lemma from [3].

Lemma 5.3. *The following holds:*

- $(F_1)_{jj} = \left(A_1^{(0)}\right)_{jj}$*, for all* $j = 1, \dots, N$*;*
- *For* $l \neq j$*, we have*

$$(F_1)_{jl} = \begin{cases} \left(A_1^{(m_j - m_l)}\right)_{jl}, & \text{if } (F_0)_{jj} = (F_0)_{ll}, \\ ((F_0)_{ll} - (F_0)_{jj}) \sum\limits_{m=-\infty}^{\infty} \frac{(A_1^m)_{jl}}{\mathrm{i}\Omega m + (A_0)_{ll} - (A_0)_{jj}}, & \text{otherwise.} \end{cases} \tag{58}$$

Proof. The first claim is proved in [3, Lemma 4.3] and the second one in [3, Lemma 4.4]. $\square$

As a direct consequence of Lemma 5.3 we can state the following theorem and corollary.

Theorem 5.4. *Let* f_0 *be a degenerate point of* F *with multiplicity* r*. Then,* F *has associated eigenvalues given by* $f_0 + \varepsilon f_i + O(\varepsilon^2)$*, where* f_i*, for* $i = 1, \dots, r$*, are the eigenvalues of the* $r \times r$ *upper-left block of* F_1 *with entries*

$$(F_1)_{lk} = \left(A_1^{(m_l - m_k)}\right)_{lk}, \quad \forall\, l, k = 1, \dots, r, \tag{59}$$

where m_l *denotes the folding number of the* l*-th eigenvalue of* A_0*.*

Proof. This theorem is proved in [3, Theorem 4.7]. $\square$

Corollary 5.5. *If the degenerate points are of order* $r = 2$ *and* $A_1^{(0)} = 0$*, then the eigenvalues* f *of* F *associated with the degenerate point* f_0 *are given by*

$$f_{1,2} = f_0 \pm \varepsilon \sqrt{(F_1)_{12}(F_1)_{21}} + O(\varepsilon^2). \tag{60}$$

Next, we seek to compute the first-order perturbation of the quasifrequencies. Note that Corollary 5.5 characterizes the perturbation of the quasifrequencies for which the non-zero Fourier coefficients of A_1 are used. Therefore, we need to compute the non-zero Fourier coefficients of M_1. As proved in [4, Theorem 5], the following asymptotic expansion of M holds if $\rho_i(t)$ and $\kappa_i(t)$ are modulated as defined in (34) with $\varepsilon_{\rho,i} = \varepsilon_{\kappa,i} = \varepsilon$, for all $1 \leq i \leq N$:

$$M_{lj} := \begin{cases} L_{lj} + \varepsilon L_{lj} \left(\cos(\Omega t + \phi_{\rho,l}) - \cos(\Omega t + \phi_{\rho,j}) \right. \\ \qquad \left. - \frac{1}{2}\left(\cos(\Omega t + \phi_{\kappa,l}) + \cos(\Omega t + \phi_{\kappa,j})\right)\right) + O(\varepsilon^2), & l \neq j, \\ L_{ll} + \varepsilon \left(\frac{\Omega^2}{2} - L_{ll}\right) \cos(\Omega t + \phi_{\kappa,l}) + O(\varepsilon^2), & l = j. \end{cases}$$

Note that the quantity $2\varepsilon\sqrt{(F_1)_{12}(F_1)_{21}}$ provides some information about the size of the band gap and in order to compute the coefficients of F_1 we need the definition of M_{lj}.

6 Physical interpretation and numerical simulations

The numerical results presented in this section are obtained for $\rho_i(t)$ and $\kappa_i(t)$ defined by (34), where we vary the parameters $\varepsilon_{\rho,i}$, $\varepsilon_{\kappa,i}$, $\phi_{\rho,i}$, $\phi_{\kappa,i}$. Note that $\varepsilon_{\rho,i} = \varepsilon_{\kappa,i} = 0$ corresponds to the static case. In the upcoming notation we omit the subscript $1 \leq i \leq N$ of a parameter, if we assume the parameter to be constant over the resonators D_i, $1 \leq i \leq N$.

Having studied the effect of small periodic perturbations of the material parameters on subwavelength quasifrequencies analytically in Section 5.2, we now want to validate these results numerically. We use the capacitance matrix approximation in order to conduct some numerical experiments under different conditions. We seek to analyze the so-called *band structure* of the material, which describes the quasifrequency-to-momentum relationship of the propagating waves [4]. We are especially interested in the occurrence of band gaps and k-gaps as a consequence of time-modulated material parameters. By definition, band gaps are the regimes of quasifrequencies with which waves cannot propagate through the material. Instead of propagating, waves with quasifrequencies in band gaps will decay exponentially. Previous work [11] has proven the occurrence of subwavelength gaps in three-dimensional high-contrast material.

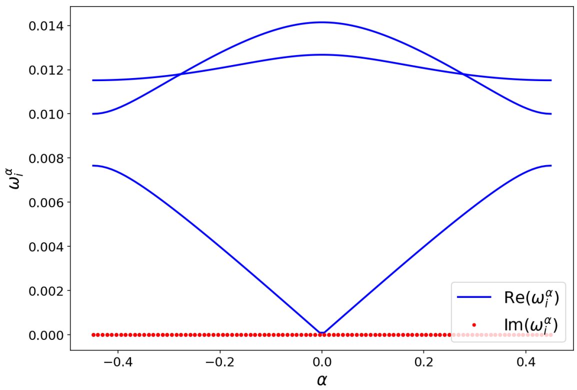

(a) We consider a setting with $\delta = 0.0001$, $\Omega = 0.03$, $v = 1$, $v_r = 1$. We assume the material parameters ρ and κ to be static, i.e., $\varepsilon_\rho = \varepsilon_\kappa = 0$.

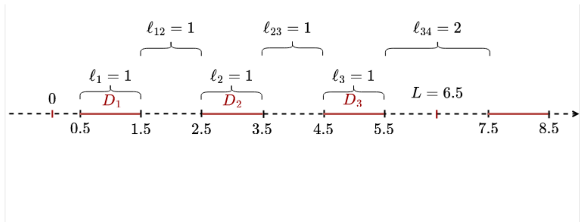

(b) Assume that the resonators in the unit cell are each of length $\ell_1 = \ell_2 = \ell_3 = 1$ with spacing $\ell_{12} = \ell_{23} = 1$, $\ell_{34} = 2$. This leads to $L = 6.5$ and $x_i^\pm$.

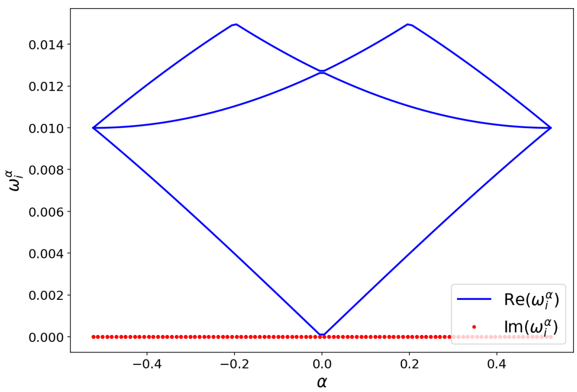

(c) We consider a setting with $\delta = 0.0001$, $\Omega = 0.03$, $v = 1$, $v_r = 1$. We assume the material parameters ρ and κ to be static, i.e., $\varepsilon_\rho = \varepsilon_\kappa = 0$.

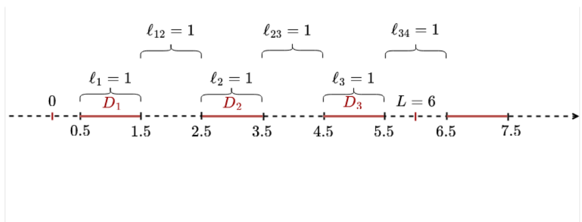

(d) Assume that the resonators are each of length $\ell_1 = \ell_2 = \ell_3 = 1$ with spacing $\ell_{12} = \ell_{23} = \ell_{34} = 1$. This leads to $L = 6$ and $x_i^\pm$.

Figure 4: Subwavelength quasifrequencies for three resonators repeated periodically in the static case. The figures on the right-hand side illustrate the setting corresponding to the numerical results shown in the left-hand side figures.

Moreover, we want to understand the effect of time-modulation on the reciprocity of wave transmission properties. The reciprocity of wave transmission is defined as follows.

Definition 6.1. We say that a wave propagates *reciprocally* if for each α in the space Brillouin zone Y^*, the quasifrequencies of the wave problem (5) at α coincide with the quasifrequencies at $-\alpha$ [4].

Note that in [3] it is proved that time-modulating the densities in a two- or three-dimensional resonator structure breaks the time-reversal symmetry of the wave propagation, which we now want to investigate in one dimension. Specifically, it has been shown in higher dimensions that time-modulating ρ turns degenerate points of the folded band structure into non-symmetric band gaps [4].

It becomes apparent from Figure 4c that there is a degenerate point at $\alpha = 0$ if the gap size between each resonator is equal, which can be treated equivalently to the case of $N = 1$ resonator in the unit cell.

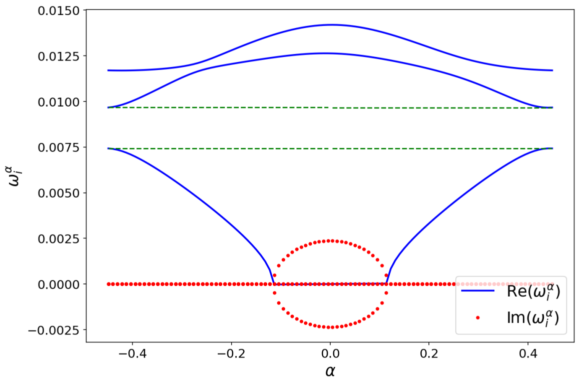

(a) Assume that ρ is time-modulated. We consider three resonators repeated periodically each of length $\ell_1 = \ell_2 = \ell_3 = 1$ with spacing $\ell_{12} = \ell_{23} = 1$, $\ell_{34} = 2$.

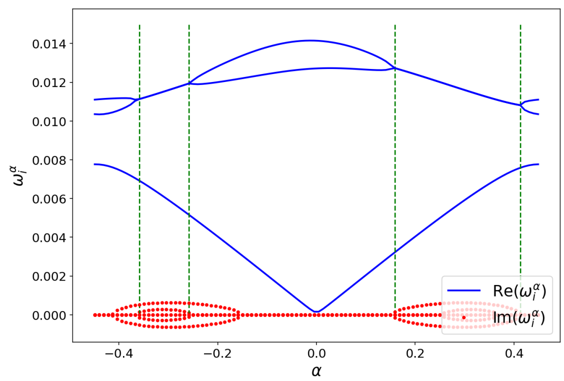

(b) Assume that κ is time-modulated. We consider three resonators repeated periodically each of length $\ell_1 = \ell_2 = \ell_3 = 1$ with spacing $\ell_{12} = \ell_{23} = 1$, $\ell_{34} = 2$.

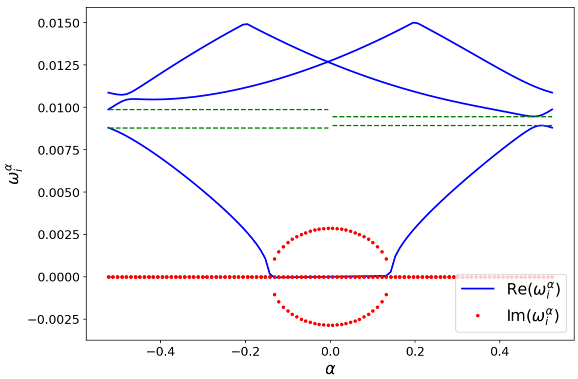

(c) Assume that ρ is time-modulated. We consider three resonators repeated periodically each of length $\ell_1 = \ell_2 = \ell_3 = 1$ with spacing $\ell_{12} = \ell_{23} = \ell_{34} = 1$.

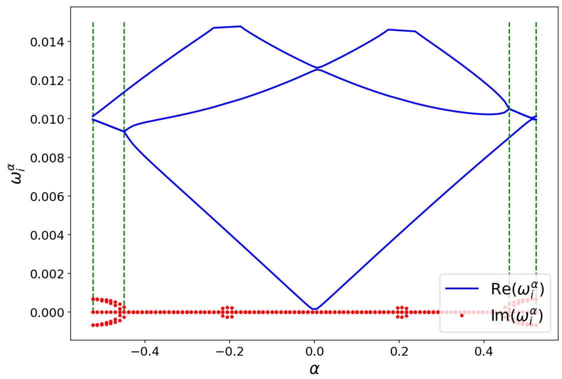

(d) Assume that κ is time-modulated. We consider three resonators each of length $\ell_1 = \ell_2 = \ell_3 = 1$ with spacing $\ell_{12} = \ell_{23} = \ell_{34} = 1$.

Figure 5: Subwavelength quasifrequencies for three resonators repeated periodically in the time-modulated case. We consider a setting with $\delta = 0.0001$, $\Omega = 0.03$, $v = 1$, $v_r = 1$. We set the amplitudes for the respective modulations to be $\varepsilon = 0.2$ with phases $\phi_1 = 0$, $\phi_2 = \pi/2$, $\phi_3 = \pi$. The green lines mark the band gaps and k-gaps.

Comparing Figure 4 with Figure 5, it becomes apparent that modulating ρ in time turns degenerate points into band gaps and modulating κ in time turns degenerate points into k-gaps.

Furthermore, measuring the size of the band gaps and k-gaps shows that the gaps forming in the regime $\alpha < 0$ do not have the same size as the gaps forming in the regime $\alpha > 0$. This means that the wave transmission is non-reciprocal in the time-modulated case. The following theorem holds true in higher dimensions [3].

Theorem 6.1. *If only the material density ρ is time-modulated, then there is a non-reciprocal band gap opening around the degenerate point.*

Proof. The proof valid in higher dimensions is still valid in one dimension due to the equivalent ODE characterization given by (50). □

The following theorem has been proven in higher dimensions in [4, Theorem 8], but can equivalently be proven in the one-dimensional case.

Theorem 6.2. *If only the material bulk κ is time-modulated, then at a degenerate point with multiplicity 2, one of the two Bloch modes is exponentially decaying and the other is exponentially increasing over time. The momentum gaps where waves exhibit this exponential behavior are called the k-gaps.*

Proof. Similar to the proof of [4, Theorem 8]. □

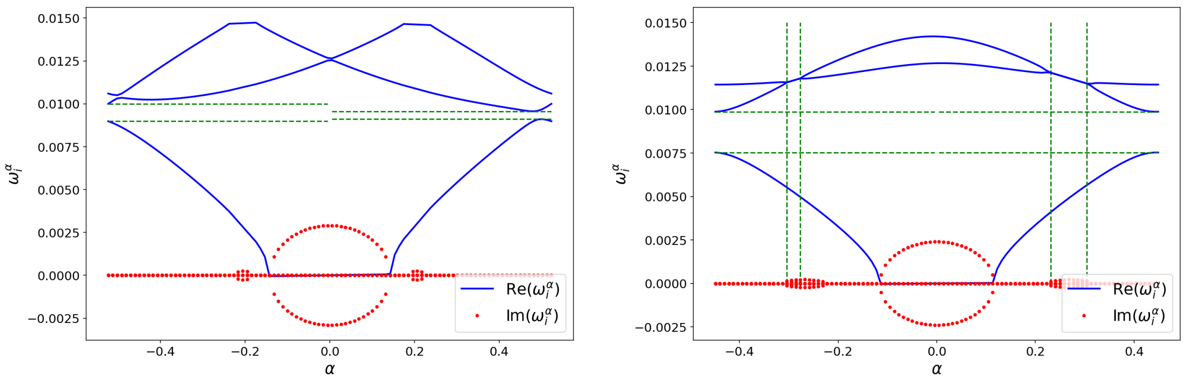

(a) We consider three resonators each of length $\ell_1 = \ell_2 = \ell_3 = 1$ with spacing $\ell_{12} = \ell_{23} = \ell_{34} = 1$.

(b) We consider three resonators each of length $\ell_1 = \ell_2 = \ell_3 = 1$ with spacing $\ell_{12} = \ell_{23} = 1$, $\ell_{34} = 2$.

Figure 6: Subwavelength quasifrequencies for three resonators in the time-modulated case. We consider a setting with $\delta = 0.0001$, $\Omega = 0.03$, $v = 1$, $v_r = 1$. We set the amplitudes for both time-modulations to be $\varepsilon = 0.2$ with phases $\phi_1 = 0$, $\phi_2 = \pi/2$, $\phi_3 = \pi$. The green lines mark the band gaps and k-gaps.

Figure 6 shows the resulting quasifrequencies if both ρ and κ are time-modulated. It can be observed that under these time-modulations, wave transmission is non-reciprocal.

7 Conclusion

In this paper we have provided the mathematical foundation to solve the quasi-periodic Helmholtz equation in one dimension with periodically time-dependent material parameters. We presented a discretization of the problem (12), which led to a scheme solving the interior problem exactly up to a negligible numerical error induced by Muller's method.

Furthermore, we have introduced a novel capacitance matrix approximation to the subwavelength quasifrequencies in one dimension assuming the problem to be quasi-periodic and the material periodically time-modulated, which is equivalent to the approximation formula valid in higher dimensions [13]. This approximation formula is advantageous because it recovers the quasifrequencies in the subwavelength range much more efficiently. Based on the capacitance matrix, the subwavelength quasifrequencies can be approximated by the formula $\omega_i^\alpha \approx v_{\mathrm{r}}\sqrt{\lambda_i^\alpha \delta}$, for all $1 \leq i \leq N$, where λ_i^α are the eigenvalues of the generalized capacitance matrix $\mathcal{C}^\alpha$. We have showed in Figure 3b that approximating the subwavelength quasifrequencies with the help of the capacitance matrix is indeed much faster than computing them with Muller's method. This observation is especially true for large values of N. We have also showed numerically that the relative error is around 0.01, which reassured the capacitance matrix approximation to be very efficient and effective.

Our numerical analysis led to the conclusion that under time-modulated material parameters, the wave transmission is non-reciprocal, which aligns with the asymptotic analysis in Section 5. Moreover, it became apparent that periodic time-modulations in the ρ_i's lead to the formation of band gaps, while periodic time-modulations in the κ_i's lead to the formation of k-gaps.

A Capacitance matrix approximation to the static problem

In this section, we recall results from [1] regarding the capacitance matrix approximation to the static problem.

Definition A.1. Consider the solution $V_i^\alpha : \mathbb{R} \to \mathbb{R}$ of the following problem:

$$\begin{cases} -\frac{\mathrm{d}^2}{\mathrm{d}x^2} V_i^\alpha = 0, & (0, L)\backslash D, \\ V_i^\alpha(x) = \delta_{ij}, & x \in D_j, \\ V_i^\alpha(x + mL) = \mathrm{e}^{\mathrm{i}\alpha mL} V_i^\alpha(x), & m \in \mathbb{Z}. \end{cases} \tag{61}$$

The corresponding capacitance matrix is defined by

$$C^\alpha_{\mathrm{static},ij} = \left.\frac{\mathrm{d}V_j^\alpha}{\mathrm{d}x}\right|_{-}(x_i^-) - \left.\frac{\mathrm{d}V_j^\alpha}{\mathrm{d}x}\right|_{+}(x_i^+) \tag{62}$$

$$= -\frac{1}{\ell_{(j-1)j}}\delta_{i(j-1)} + \left(\frac{1}{\ell_{(j-1)j}} + \frac{1}{\ell_{j(j+1)}}\right)\delta_{ij} - \frac{1}{\ell_{j(j+1)}}\delta_{i(j+1)}$$

$$- \delta_{1j}\delta_{iN}\frac{\mathrm{e}^{-\mathrm{i}\alpha L}}{\ell_{N(N+1)}} - \delta_{1i}\delta_{jN}\frac{\mathrm{e}^{\mathrm{i}\alpha L}}{\ell_{N(N+1)}}, \tag{63}$$

or equivalently by

$$C^\alpha_{\mathrm{static}} = \begin{bmatrix} \frac{1}{\ell_{N(N+1)}} + \frac{1}{\ell_{12}} & -\frac{1}{\ell_{12}} & & & -\frac{\mathrm{e}^{-\mathrm{i}\alpha L}}{\ell_{N(N+1)}} \\ -\frac{1}{\ell_{12}} & \frac{1}{\ell_{12}} + \frac{1}{\ell_{23}} & -\frac{1}{\ell_{23}} & & \\ & \ddots & \ddots & \ddots & \\ & & \ddots & \ddots & -\frac{1}{\ell_{(N-1)N}} \\ -\frac{\mathrm{e}^{\mathrm{i}\alpha L}}{\ell_{N(N+1)}} & & & -\frac{1}{\ell_{(N-1)N}} & \frac{1}{\ell_{(N-1)N}} + \frac{1}{\ell_{N(N+1)}} \end{bmatrix}. \tag{64}$$

The following asymptotics of the band functions hold.

Proposition A.1. *The first N subwavelength band functions are approximately given by*

$$\omega_i^\alpha = \sqrt{\delta \lambda_i^\alpha} + O(\delta) \tag{65}$$

as $\delta \to 0$, where λ_i^α are the eigenvalues of the generalized capacitance matrix

$$\mathcal{C}^\alpha_{\text{static}} := V^2 L^{-1} C^\alpha_{\text{static}}.$$

Here, $V := \operatorname{diag}((v_i))$ and $L := \operatorname{diag}((\ell_i))$.

References

[1] Habib Ammari, Silvio Barandun, Jinghao Cao, and Florian Feppon. Edge modes in subwavelength resonators in one dimension. *arXiv preprint arXiv:2301.06747*, 2023.

[2] Habib Ammari and Jinghao Cao. Unidirectional edge modes in time-modulated metamaterials. *Proc. Royal Soc. A*, 478:2022.0395, 2022.

[3] Habib Ammari, Jinghao Cao, and Erik Orvehed Hiltunen. Non-reciprocal wave propagation in space-time modulated media. *Multiscale Model. Simul.*, 20(4):1228–1250, 2022.

[4] Habib Ammari, Jinghao Cao, and Xinmeng Zeng. Transmission properties of space-time modulated metamaterials. *Stud. Appl. Math.*, pages 1–24, 2023.

[5] Habib Ammari, Bryn Davies, and Erik Orvehed Hiltunen. Functional analytic methods for discrete approximations of subwavelength resonator systems. *arXiv preprint arXiv:2106.12301*, 2021.

[6] Habib Ammari, Bryn Davies, and Erik Orvehed Hiltunen. Robust edge modes in dislocated systems of subwavelength resonators. *J. London Math. Soc.*, 106(3):2075–2135, 2022.

[7] Habib Ammari, Bryn Davies, Erik Orvehed Hiltunen, and Sanghyeon Yu. Topologically protected edge modes in one-dimensional chains of subwavelength resonators. *J. Math. Pures Appl.*, 144:17–49, 2020.

[8] Habib Ammari, Francesco Fiorani, and Erik Orvehed Hiltunen. On the validity of the tight-binding method for describing systems of subwavelength resonators. *SIAM J. Appl. Math.*, 82(4):1611–1634, 2022.

[9] Habib Ammari, Brian Fitzpatrick, David Gontier, Hyundae Lee, and Hai Zhang. Minnaert resonances for acoustic waves in bubbly media. *Ann. Inst. H. Poincaré C Anal. Non Linéaire*, 35(7):1975–1998, 2018.

[10] Habib Ammari, Brian Fitzpatrick, Hyeonbae Kang, Matias Ruiz, Sanghyeon Yu, and Hai Zhang. *Mathematical and Computational Methods in Photonics and Phononics*, volume 235 of *Mathematical Surveys and Monographs*. American Mathematical Society, Providence, RI, 2018.

[11] Habib Ammari, Brian Fitzpatrick, Hyundae Lee, Sanghyeon Yu, and Hai Zhang. Subwavelength phononic bandgap opening in bubbly media. *J. Differential Equations*, 263(9):5610–5629, 2017.

[12] Habib Ammari, Erik O. Hiltunen, and Thea Kosche. Asymptotic floquet theory for first order odes with finite fourier series perturbation and its applications to floquet metamaterials. *J. Differential Equations*, 319:227–287, 2022.

[13] Habib Ammari and Erik Orvehed Hiltunen. Time-dependent high-contrast subwavelength resonators. *J. Comput. Phys.*, 445:110594, 2021.

[14] Habib Ammari, Bowen Li, and Jun Zou. Mathematical analysis of electromagnetic scattering by dielectric nanoparticles with high refractive indices. *Trans. Amer. Math. Soc.*, 376(1):39–90, 2023.

[15] Habib Ammari, Pierre Millien, Matias Ruiz, and Hai Zhang. Mathematical analysis of plasmonic nanoparticles: the scalar case. *Arch. Ration. Mech. Anal.*, 224(2):597–658, 2017.

[16] Habib Ammari and Hai Zhang. A mathematical theory of super-resolution by using a system of sub-wavelength helmholtz resonators. *Comm. Math. Phys.*, 337(1):379–428, 2015.

[17] Kazunori Ando and Hyeonbae Kang. Analysis of plasmon resonance on smooth domains using spectral properties of the neumann-poincaré operator. *J. Math. Anal. Appl.*, 435(1):162–178, 2016.

[18] Kazunori Ando, Hyeonbae Kang, and Hongyu Liu. Plasmon resonance with finite frequencies: a validation of the quasi-static approximation for diametrically small inclusions. *SIAM J. Appl. Math.*, 76(2):731–749, 2016.

[19] R. Carminati, A. Cazé, D. Cao, F. Peragut, V. Krachmalnicoff, R. Pierrat, and Y. De Wilde. Electromagnetic density of states in complex plasmonic systems. *Surface Science Reports*, 70(1):1–41, 2015.

[20] Youjun Deng, Hongjie Li, and Hongyu Liu. Analysis of surface polariton resonance for nanoparticles in elastic system. *SIAM J. Math. Anal.*, 52(2):1786–1805, 2020.

[21] Florian Feppon and Habib Ammari. Subwavelength resonant acoustic scattering in fast time-modulated media. *HAL preprint hal-03659025.*, 2022.

[22] Florian Feppon, Zijian Cheng, and Habib Ammari. Subwavelength resonances in 1D high-contrast acoustic media. *SIAM J. Appl. Math.*, 2023.

[23] Emanuele Galiffi, Romain Tirole, Shixiong Yin, Huanan Li, Stefano Vezzoli, Paloma A. Huidobro, Mário G. Silveirinha, Riccardo Sapienza, Andrea Alù, and J. B. Pendry. Photonics of time-varying media. *Advanced Photonics*, 4(1):014002, 2022.

[24] Hao Ge, Min Yang, Chu Ma, Ming-Hui Lu, Yan-Feng Chen, Nicholas Fang, and Ping Sheng. Breaking the barriers: advances in acoustic functional materials. *National Science Review*, 5:159–182, 2018.

[25] F.D.M. Haldane and S. Raghu. Possible realization of directional optical waveguides in photonic crystals with broken time-reversal symmetry. *Phys. Rev. Lett.*, 100(1):013904, 2008.

[26] Fabrice Lemoult, Mathias Fink, and Geoffroy Lerosey. Acoustic resonators for far-field control of sound on a subwavelength scale. *Phys. Rev. Lett.*, 107:064301, 2011.

[27] Fabrice Lemoult, Nadège Kaina, Mathias Fink, and Geoffroy Lerosey. Soda cans metamaterial: A subwavelength-scaled phononic crystal. *Crystals*, 6(7):82, 2016.

[28] Valentin Leroy, Alice Bretagne, Mathias Fink, Hervé Willaime, Patrick Tabeling, and Arnaud Tourin. Design and characterization of bubble phononic crystals. *Appl. Phys. Lett.*, 95(17):171904, 2009.

[29] Hongjie Li, Hongyu Liu, and Jun Zou. Minnaert resonances for bubbles in soft elastic materials. *SIAM J. Appl. Math.*, 82(1):119–141, 2022.

[30] Junshan Lin and Hai Zhang. Mathematical theory for topological photonic materials in one dimension. *J. Phys. A*, 55(49):495203, 2022.

[31] Guancong Ma and Ping Sheng. Acoustic metamaterials: From local resonances to broad horizons. *Science Advances*, 2(2):e1501595, 2016.

[32] Taoufik Meklachi, Shari Moskow, and John C. Schotland. Asymptotic analysis of resonances of small volume high contrast linear and nonlinear scatterers. *J. Math. Phys.*, 59(8):083502, 2018.

[33] M. Minnaert. On musical air-bubbles and the sounds of running water. *Phil. Mag.*, 16(104):235–248, 1933.

[34] S. Raghu and F.D.M. Haldane. Analogs of quantum-hall-effect edge states in photonic crystals. *Phys. Rev. A*, 78:033834, 2008.

[35] Dimitrios L. Sounas and Andrea Alù. Non-reciprocal photonics based on time modulation. *Nature Photonics*, 11:774–783, 2017.

[36] Sajjad Taravati and Ahmed A. Kishk. Space-time modulation: Principles and applications. *IEEE Microwave Magazine*, 21(4):30–56, 2020.

[37] Gerald Teschl. *Ordinary Differential Equations and Dynamical Systems.* American Mathematical Society, 2012.